Hydroxypropyl Methylcellulose Nanocomposites Containing Nano Fibrillated Cellulose (NFC) from *Agave americana* L. for Food Packaging Applications

Paladugu Krishnadev,[a] Kizhaeral S. Subramanian,[b,*] Arunachalam Lakshmanan,[a] Shunmugam Ganapathy,[c] Kalimuthu Raja,[a] and Subramania Krishnaraj Rajkishore [d]

Hydroxypropylmethylcellulose (HPMC) is popularly known as a hydrocolloid for potential use as a biopolymer film. The films of HPMC exhibit brittleness, lacking flexibility, but they can provide a gas barrier. With the aim of improving the HPMC film properties, nanofibrillated cellulose (NFC) from the succulent plant *Agave americana* L was incorporated as reinforcement material using the solution casting method. The films were prepared with three different amounts of NFC with glycerol as a plasticizer. The incorporation of the NFC into the nanocomposite films showed a 1,000-fold reduction in the gas permeability. However, significant improvements in the tensile strength (TS), the elongation at break (EAB), and Young's modulus (YM) were only observed with 1% NFC. A higher moisture content (24.5%) and a higher solubility (59.5%) were observed in the HPMC/NFC-1 film, which also exhibited the best biodegradability loss of the films that were observed with a 92.8% degradation rate in 15 d of soil burial studies. Therefore, the results evidence that the HPMC/NFC films might be potentially suitable as food wrap packaging on perishable produce of fruits and vegetables to maintain their quality attributes and prolong the storage life.

Keywords: Hydroxypropyl methylcellulose; Nanofibrillated cellulose; Nanocomposite films; Mechanical properties; Barrier properties

Contact information: a: Department of Nano Science & Technology, Tamil Nadu Agricultural University, Coimbatore-641003, Tamil Nadu, India; b: Director of Research, Tamil Nadu Agricultural University, Coimbatore-641003, Tamil Nadu, India; c: Department of Food & Agricultural Process Engineering, Tamil Nadu Agricultural University, Coimbatore-641003, Tamil Nadu, India; d: Department of Environmental Sciences, Tamil Nadu Agricultural University, Coimbatore-641003;
** Corresponding author: kss@tnau.ac.in*

INTRODUCTION

Presently, there is great attention from people throughout the world on various issues associated with environmental conservation. This has spurred a push to utilize eco-friendly agricultural waste. Such biomass is underutilized, particularly in India, which is the second-largest agricultural nation after China (Chandra *et al*. 2012). The term "packaging" is commonly used to define a material that can protect various food products from physical, chemical, and biological damage. Recently, the use of petroleum-based plastic materials is widely under attack due to improper recycling facilities or lack of infrastructure, non-biodegradability, non- renewability, non-recyclability, or addition of toxic additives.

Currently, the total share of plastics in the food packaging sector accounts (85%). The global perspective in the packaging market increased the revenues from $42.5 billion in 2014 to nearly $48.3 billion by 2020 (Huang *et al.* 2020). Plastics are the most widely

preferred packaging materials, due to their light weight, good processability, good mechanical and barrier properties, and low-cost production (Sangroniz *et al.* 2019). The market growth rate of plastic packaging has been expanding by 20 to 25% per year (Huang *et al.* 2020). However, there is an environmental concern against single-use plastics (SUP), which is harmful to human health and aquatic life (Halimatul *et al*. 2019). In general, though many plastics that are made of petroleum-based packaging are technically recyclable, they instead are cast out as litter. They are mostly used by consumers for a short period, but then take centuries to degrade in natural ecosystems (The European Parliament and the Council of the European Union 2019). Additionally, the recycling of packaging waste has a target of a minimum of 70% by weight and about 55% for plastic, by the end of 2030 (The European Parliament and the Council of the European Union, 2018). However, recycling rates still were low in 2017 in some of the countries. The recycling percentage of plastics packaging according to the European Union is 41.7% (Eurostat, 2018). Furthermore, the most commonly followed process for impacting the final properties of the plastics is mechanical recycling (Geyer *et al*. 2017). Since 1950, the amount of plastic waste generated is about 6300 million tons, of which 4977 million tons are mostly accumulated in waterways and landfills (De Souza Machado *et al*. 2018). Microplastics (< 5.0 mm) is another major and emerging problem that is present in the water, air, and soil, which gives harmful effects on both marine and terrestrial ecosystems (Geyer *et al*. 2017). In response, the global biodegradable polymer market is expected to grow in revenues from $3.1 billion in 2016 to $7.1 billion by 2021, an annual growth rate of 18% (Huang *et al.* 2020).

Scientists across the various disciplines are working to find an alternative way to produce polymers from green sources to resolve the negative effects of petroleum-based polymers. Thermoplastic starch-based films are among some of the environmentally friendly alternatives to petroleum-based plastics. Research has shown that thermoplastic starch films can possess incredible reinforcing properties with the capability to modify or blend with other suitable polymers. This can facilitate the mass production of economical and biodegradable packaging materials (Sanyang *et al.* 2017; Ilyas *et al.* 2018; Atikah *et al.* 2019). Hydroxypropyl methylcellulose (HPMC) is one of the cellulose derivatives next to cellulose, cellulose diacetate, and cellulose triacetate. Hydroxypropyl methylcellulose is composed of units of β (1-4)-D-glucose linked by glycosidic bonds, and it is extensively used to produce edible films and coatings for packaging purposes. In addition, HPMC is used as an emulsifier, stabilizing, suspending, and gelling agent in the food industry (Burdock 2007). Hydroxypropyl methylcellulose is soluble in cold water and forms transparent, tasteless, odorless, flexible, and tough films from the film solutions (McGinity and Felton 2008). It is widely employed because of its abundance, good water solubility, non-toxic nature, and rapid processability (Ford 1999). Additives such as glycerol are incorporated into films with HPMC to improve the overall performance and properties (Navarro-Tarazaga *et al*. 2008).

Generally, glassy HPMC film surfaces are highly hydrophilic, which causes water molecules from the surroundings to induce both swelling and reduction in glass transition temperature, and this happens when temperature and humidity are combined (Laksmana *et al*. 2009). Moreover, the films tend to dissolve and flow. Another valid explanation is that when the films are exposed to high humidity, there is a reduction in breakdown strength and increased losses (Hui *et al.* 2013).

Interest in polymer nanocomposites has been recently ignited because of their use in the food packaging sector. Nano-biopolymers such as nanofibrillated cellulose (NFC),

and nanocrystalline cellulose (NCC) are derived from various plant sources. Such nanocellulose (NC) materials can be reinforced into a polymer matrix that exhibits good physicochemical properties and does not negatively affect the environment (Iyer *et al.* 2015b; Iyer and Torkelson 2015; Yang *et al.* 2015; Dimic-Misic *et al.* 2017). Nanocomposites derived from plant materials can provide outstanding and unique properties that are not found in conventional composites. Nanofibrillated cellulose is derived naturally from various plant fibers, such as agave, sisal, banana pseudostem, pineapple, jute, hemp, and cotton (Ramesh *et al*. 2017). These cellulose biopolymers are transformed from micro to nanoscale fibrils with a long, flexible, entangled, and web-like network with a mean diameter of 1 nm to 100 nm (Krishnadev *et al*. 2020). Nano biopolymers are great candidates for food packaging applications due to their unique (Du *et al.* 2016; Li *et al*. 2016), biological (Wang *et al*. 2015), and physical properties (Yang *et al.* 2015; Cui *et al*. 2016). In particular, numerous studies on NFC as a reinforcing agent in the polymer matrix, which has been widely researched worldwide in past decades, have shown potential for food packaging applications. The prepared bio-films showed good mechanical robustness and improvement of cohesion and the homogenous surface of the films. Hay *et al*. (2018) successfully formulated HPMC by incorporating amylose-sodium palmitate inclusion complexes (Na-Palm) using the conventional solution casting method. The films had improved physical barrier and gas properties compared to the HPMC films. In addition to reducing the water vapor and oxygen permeability traits, the treated films improved the elongation at break (EAB), Young's modulus (YM), and tensile strength (TS) values. Ilyas *et al.* (2019) prepared and studied the effect of NFC from the mixture leaves of sugar palm and sugar palm starch (SPS) by the casting method. The films with smaller diameters demonstrated strong miscibility, compatibility, and water barrier properties. Cheng *et al.* (2018) studied the preparation and extraction of nanofibrillated acetylated cellulose from corn stalk by chemical-mechanical processes and studied the reinforcement effect on starch films. The uniform dispersal of nano-fillers in the starch composite films showed greater tensile strength performances. Associated works on NFC-reinforced biopolymer nanocomposites will help promote the development of environmentally friendly and biodegradable packing films with good physical and mechanical properties.

Agave americana L. is known for its strong and rigid natural succulent plant fibers which are found in dry arid areas in India; it belongs to the Asparagaceae family (Krishnadev *et al.* 2020). Agave fibers have some unique characteristics such as high moisture, low density, and high tensile strength. Fresh leaves of *A. americana* contain approximately 60% to 80% cellulose. Cellulose has a micro-fiber structure with different types of chemical bonds such as covalent, hydrogen, or van der Waals bonds (Chaabouni *et al.* 2006). Therefore, cellulose has a strong potential for reinforcement in polymer composite materials.

In this study, NFC was used as a reinforcing filler for making biodegradable, flexible, and transparent HPMC/NFC composite films. The role of NFC as a reinforcement of the structural, thermal, barrier, and mechanical properties of the HPMC/NFC films was performed systematically. The nanocomposite films were assessed for their tensile strength (TS), EAB, and YM values. A gas permeability test (GPT) was also used to measure the mechanical and barrier properties in the biodegradable films. The functional and structural interaction of the HPMC/NFC films was performed by using Fourier transform infrared spectroscopy (FTIR) and X-ray diffraction (XRD). The surface morphology was studied *via* scanning electron microscopy (SEM) to determine the HPMC/NFC composite films. The rheological properties of the HPMC/NFC composite films were extensively studied to

understand the role of NFC in the formulation of the prepared films. The moisture content, water solubility, and biodegradability test of commercial polyvinyl chloride (PVC) and nanocomposite films were also studied. This demonstration was done in consideration of using NFC in polysaccharide films to address the demands of food packaging applications.

EXPERIMENTAL

Materials

The HPMC (M_w of 1261.45) was sourced from HiMedia Laboratories (Mumbai, India), while the glycerol (M_w of 92.09) was sourced from S.D. Fine-Chem Limited (Mumbai, India). Distilled and Millipore water was sourced from the Department of Nano Science and Technology (Tamil Nadu Agricultural University, Coimbatore, India). The commercial PVC (Oxywrap Cling Film; Paradise Consumer Products Ltd., Jalgaon, India) was purchased from the local market for comparative study along with the nanocomposite films.

Methods

Source of cellulose

The nanocellulose was prepared from *Agave americana*. L plant fiber, which was collected from the Thondamuthur village of Coimbatore city in Tamil Nadu, India. The fibers are successfully treated subsequently for alkali, bleaching, and acid hydrolysis to obtain nanocellulose. The complete methodology for cellulosic fibers extraction and transformation of microfibrils to nanofibrils was successfully carried out and reported in the authors' previous work (Krishnadev *et al*. 2020). The obtained nanocellulose is used for the processing of nanocomposite films as a natural reinforcing filler material.

Preparation of the NFC from the Agave americana L.

The cellulosic fibers suspension was transferred to a petri dish and allowed to dry under a hot air oven at 60 °C for 3 h to evaporate the moisture, as shown in Fig. 1. Concurrently, 1 g (w/w) of dry cellulosic fibers mass was redistributed in 100 mL of distilled water under steady vigorous magnetic agitation for 3 h, followed by an ultra-sonication bath using a CD 4820 2.5 L digital ultrasonic cleaner (Citizen Scales, Mumbai, India) for 30 min to obtain nanofibrillated cellulose. The solids content of the NFC was estimated in a set of three by collecting 10 mL, 15 mL, and 20 mL samples from 100 mL of the liquid NFC suspension, which was allowed to dry under a hot air oven at 60° C for 5 h. The NFC suspension was hermetically sealed and stored in a refrigerator at 5 °C for subsequent use.

Preparation of the HPMC/NFC nanocomposite films

The HPMC/NFC composite film preparation procedure is shown in Fig. 1. Initially, HPMC powder was dissolved in 100 mL distilled water and stored in a refrigerator for 14 h at 5° C. Furthermore, constant stirring under a magnetic stirrer was allowed to produce a homogeneous film formulation at addition levels of 1%, 2%, and 3% (w/v) (Fig. 2b). The NFC liquid suspension prepared after homogenization followed by an ultrasonic bath is shown in Fig. 2a.

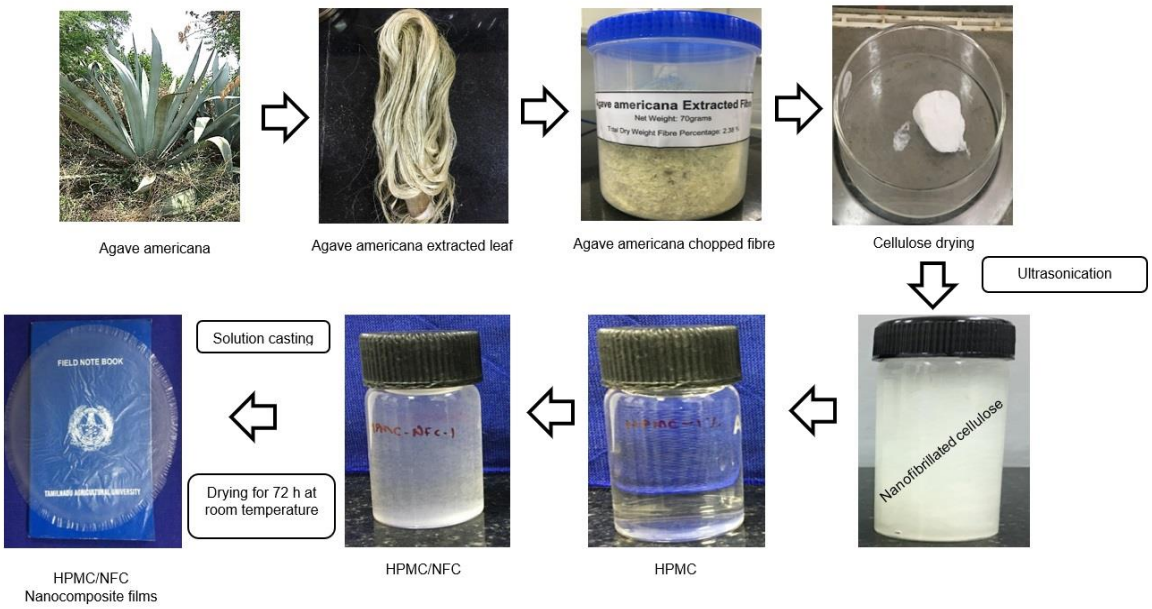

Fig. 1. Preparation steps for the HPMC/NFC nanocomposite films

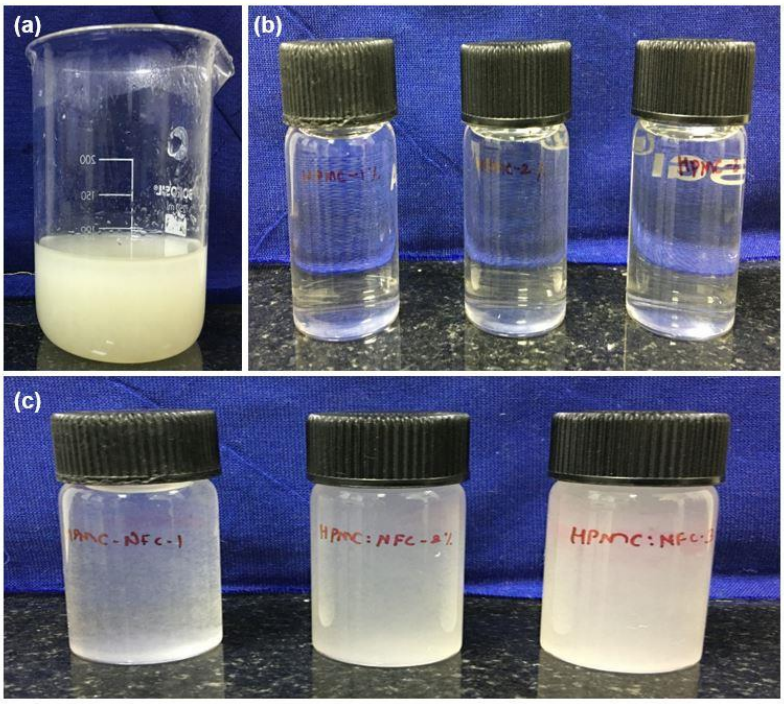

Fig. 2. Digital images for the a) NFC formulation, the b) Different amounts of the HPMC formulation, and the c) HPMC/NFC formulation with different amounts of NFC

The NFC solids content for final optimization was successful in mixing 10 mL (0.053%), 15 mL (0.043%), and 20 mL (0.091%) of the NFC liquid suspension in 89 mL, 84 mL, and 79 mL of the HPMC formulation, respectively. One mL of glycerol was incorporated as a plasticizer and blended completely at 600 rpm for 1 h to obtain the final

HPMC/NFC mixture at concentrations of 1%, 2%, and 3% (Fig. 2c). Subsequently, 100 mL of the final film composite of pure HPMC and HPMC/NFC final composite film was poured onto food-grade polypropylene (PP) round plastic plates with dimensions of 27.3 cm × 27.3 cm × 2.2 cm for forming nanocomposite films. The films were peeled carefully after 48 to 72 h of solvent casting at room temperature 35° C ± 72%. Moreover, all the peeled films had a uniform thickness and were stored in a plastic file for the morphological, structural, functional, barrier, mechanical, thermal degradation, moisture content, water solubility, and soil burial-based biodegradability tests.

Measurement of the moisture content

To determine the weight loss of the films, the moisture content was estimated. The HPMC and HPMC/NFC films were cut into square 2.0 cm^2 × 2.0 cm^2 pieces. The initial weight of all the films was weighed accurately. The final dry mass was recorded upon drying in an oven at 100 °C for 120 min to acquire the final dry weight. Each film treatment was replicated five times, and the moisture content was measured according to Eq. 1 (Kim *et al.* 2017),

$$\textit{Moisture Content (\%)} = \left[\frac{(Wi - Wf)}{Wi}\right] \times 100 \quad (1)$$

where W_i is the initial weight taken at the beginning and W_f is the final weight after the film was dried in the oven.

Measurement of solubility in water

All the film samples were cut into square 2.0 cm^2 × 2.0 cm^2 pieces. The samples were weighed before they were immersed in 100 mL of distilled water for 24 h at ambient room conditions with minimal modifications (Ghasemlou *et al*. 2013). After they were removed from the water, the samples were dried in a hot air oven at 100 °C until the final weight did not decrease. The final dry weight of all the samples was accurately weighed and recorded. Glycerol incorporated as a plasticizer into the film has a good water solubility range from 18% to 25% (Gáspár *et al.* 2005). The percentage of water solubility was calculated according to Eq. 2,

$$\textit{Solubility (\%)} = \left[\frac{(Mo - Mi)}{Mo}\right] \times 100 \quad (2)$$

where M_o is the initial dry weight taken at room temperature and M_i is the final dry weight of the films at 100 °C in the oven.

Biodegradability test

The biodegradation process of the commercial PVC (Cling film), and the prepared films was determined by the frequently used soil burial method with minimal modifications (Marichelvam *et al.* 2019). The soil was procured from the experimental field at Tamil Nadu Agricultural University, Coimbatore, Tamil Nadu, India. Approximately 200 g of soil was placed in series of disposable paper cups with dimensions of 9 cm × 7.5 cm × 9 cm. The 2 cm × 2 cm film samples were buried at depth of 2 cm for 15 d. All the cups were incubated at ambient room conditions (25 °C to 35 °C), and the moisture content of the soil was maintained at 35% to 40% by sprinkling water twice a day. The degradation of the samples was successfully determined at 7 d intervals by carefully taking samples from the soil. The degradation measurements were assisted by polypropylene wipes moistened with

distilled water to remove the soil. The sample was dried in the oven until a constant weight was obtained. The final biodegradability weight loss was calculated according to Eq. 3,

$$\textit{Weight Loss (\%)} = \left[\frac{(Wo-W)}{Wo}\right] \times 100 \quad (3)$$

where W_o is the weight of the samples before the test and W is the weight of samples after the test.

Characterization and Analysis

Rheological behavior measurement of the nanocomposite formulations

The rheological behavior of the composite HPMC/NFC films was measured with an advanced cylinder rotating rheometer device (MCR52; Anton Paar, Graz, Austria). Approximately 2 mL of film solution was poured over the sample load and the test was measured. The shear rate varied from 1 s^{-1} to 100 s^{-1}. All the film formulations were carried out using the computer-based master tool software RheoPlus (Anton Paar, Graz, Austria), which was the default automatic measuring and detection system connected to the rheometer.

Ultraviolet-visible spectroscopy (UV-Vis) transmittance studies

Ultraviolet-visible spectroscopy studies were carried out to better understand the UV transmitting properties of the commercial PVC (Cling Film) and the HPMC/NFC nanocomposite films. A double beam UV spectrophotometer (Genesys 180; Thermo Fisher Scientific, Waltham, MA, USA) was used to determine the UV transmitting properties. The film samples were cut into 40 mm × 10 mm pieces, and the samples were placed in the cuvette for UV irradiation that was emitted *via* xenon flash lamp. Millipore water (Department of Nano Science and Technology, Tamil Nadu Agricultural University, Coimbatore, India) was used as a blank. The spectra were acquired from 200 to 800 nm.

Fourier transform infrared spectroscopy (FTIR)

The FTIR spectrums of the nanocomposite film samples were recorded using a Jasco FT/IR-6800 spectrometer (Tokyo, Japan). The uniform circular size of all the film samples was punched using a stationary paper punching machine. The samples were placed on attenuated total reflection (ATR) and the scanning accumulation was performed with 64 scans and a spectral range of 4000 cm^{-1} to 400 cm^{-1} for each film sample.

X-ray diffraction (XRD)

The XRD patterns of the HPMC/NFC composite films were recorded using a Rigaku Ultima IV diffractometer (Tokyo, Japan) in a scattering range of 2θ (10° to 90°) at a scanning speed of 10 °/min. All the samples were cut to 2 cm × 2 cm, placed on the XRD glass quartz sample holder, and measured at 40 kV and 30 mA at room temperature and humidity.

Thermogravimetric analysis (TGA)

The thermogravimetric analysis (TGA) of the HPMC and HPMC/NFC composite films at different concentrations of HPMC was conducted using an EXSTAR TG-DTA SII 6300 instrument (Tokyo, Japan). All the film samples were studied under a nitrogen gas atmosphere to prevent thermo-oxidative degradation. Approximately 10 mg of the composite films were scanned from 23 °C to 430 °C at a heating rate of 10 °C/min.

Surface morphology observation of the nanocomposite films

The different concentrations of the pure HPMC and HPMC/NFC composite films were observed using a Quanta 250 SEM (FEI, Hillsboro, OR, USA) at an accelerating voltage of 10.00 kV at ambient temperature. All the film samples were cut at a uniform size and placed on a conductive tape sample stub and sputter-coated (Emitech SC7620; Quorum Technologies, East Sussex, UK) with gold and palladium directly to avoid charging.

Determination of the mechanical properties of the nanocomposite films

The HPMC and HPMC/NFC composite film samples were cut into rectangular pieces (10 mm wide × 100 mm long) before the TS, EAB, and YM values of the nanocomposite films were determined using a universal testing machine (Model No. 9052; Dak System Inc., Mumbai, India), according to the ASTM standard D882-18 (2018). The flaring area on both ends was adjusted to a 25 mm × 50 mm grip. The film samples were successfully mounted to the testing machine extension grips and the crosshead speed was set to 100 mm and the stretching rate was 50 mm/min.

Gas permeability measurement of the nanocomposite films

For the gas permeability testing (GPT) of the HPMC and HPMC/NFC films, the samples were cut to 100 mm × 100 mm pieces according to the ISO standard 15105-1 (2007). The gas permeation was performed using a manometric gas permeability tester (Lyssy L100-500; Systech Illinois, Johnsburg, IL, USA). The samples were placed carefully on the gas chamber column, and the upper and lower pressure limits were adjusted at 700 and 500 psi at a temperature of 25 °C. The results were expressed in mL/m^2 per day.

RESULTS AND DISCUSSION

Moisture Content Measurement of the HPMC/NFC Nanocomposite Films

The moisture content for the commercial PVC (Cling film), the HPMC, and the HPMC/NFC films were calculated, as shown in Table 1. The results showed that there was no water adsorption in the commercial PVC film. However, the HPMC-1, HPMC-2, and HPMC-3 films showed lower moisture contents of 4%, 13%, and 9%, compared to the HPMC/NFC-1, HPMC/NFC-2, and HPMC/NFC-3 films, which had moisture contents of 25%, 19%, and 22%, respectively. It is known that NFC derived from *Agave americana* fiber has a higher moisture content (Msahli *et al.* 2015). The increase in the film solubility is because of the strongly hydrophilic nature of the NFC. However, a proportional decrease would be due to the hydrophobic compounds (Kavoosi *et al*. 2013). From this, it can be concluded that the moisture content from the samples had the lowest value trend. Finally, the HPMC/NFC-1 sample possessed the ability to enhance the shelf life of the film for further applications.

Water Solubility Measurement of the HPMC/NFC Nanocomposite Films

The water solubility measurement of film gives important characteristics and quality of food products in packaging materials. It is closely related to the biodegradation properties of the films. From the results shown in Table 1, the lowest water solubility (6.7%) was observed in the commercial PVC sample. The HPMC samples had higher water solubility for the HPMC-1, HPMC-2, and HPMC-3 films at 63%, 46%, and 56%,

respectively. The HPMC/NFC nanocomposite samples had slightly lower water solubility in the HPMC/NFC-1, HPMC/NFC-2, and HPMC/NFC-3 films at 59%, 40%, and 37%, respectively. The water solubility values in the HPMC/NFC films may have been attributed to the strong water holding capacity in the NFC. Furthermore, various hydrocolloid-based biopolymers, which are largely employed as food packaging materials, should be very sensitive to moisture. Otherwise, there is a chance of losing the physical efficiency of the film material, as well as the inability to prevent microbial attack and chemical spoilage inside the food products (Hosseini *et al.* 2021). Another valid explanation is that the addition of the plasticizers may have reduced the polymer molecule interaction by providing a larger space in which the water molecules could be penetrated, thus maximizing the solubility of the nanocomposite films (Ibrahim *et al*. 2019). Finally, film materials with high water solubility can be used in single-use biodegradable packaging applications (Preechawong *et al.* 2005; Cai *et al.* 2011; Lv *et al.* 2018).

Biodegradability Properties of the HPMC/NFC Nanocomposite Films

Biodegradation of the polymer material occurs when the material is degraded or broken down into constituent molecules by natural processes. Among biodegradation methods, soil burial is a very frequently followed method to determine the total biodegradability loss of polymer films over a 15-d period, over which the samples are placed at a depth of 2 cm in the soil. The film's weight loss was determined based on the total amount of degradation that could be taken as an indicator in natural soil. The results from the soil degradation test are shown in Table 1. A biodegradation weight loss of 14% was observed in the commercial PVC (Cling film), followed by 9%, 25%, and 25% in the HPMC-1, HPMC-2, and HPMC-3 samples, respectively. The surface of the film was visualized and found that there is a loss of surface uniformity, smoothness, and even a few samples are more brittle which are broken into pieces (Marichelvam *et al.* 2019). The biodegradation losses increased at the initial stages and then decreased in the HPMC/NFC-1, HPMC/NFC-2, and HPMC/NFC-3 films with values of 93%, 32%, and 24%, respectively compared to the commercial PVC and HPMC films. It is strongly understood that the film materials are highly hydrophilic, which favors more water absorption in the water activity of the nanocomposite films. Glycerol, which was used as a plasticizer, could have caused the adsorption by soil, water penetration through the cell membrane, and weight loss of the films, among other things. Another valid explanation is that the rates of degradation in films can be attributed to environmental factors, such as temperature, moisture, and biological activity (Maran *et al.* 2014). From this research, it was concluded that the soil burial depth showed a gradual weight loss during biodegradation of the films.

Table 1. Mean Values of the Moisture Content, Water Solubility, and Biodegradability Test of the PVC, HPMC, and HPMC/NFC films

Sample	Moisture Content (%)	Water Solubility (%)	Biodegradability Loss (%)
Commercial PVC Cling Film	0 ± 0.00	6.66 ± 0.00	14.28 ± 0.002
HPMC-1	3.7 ± 0.006	62.96 ± 0.004	9.09 ± 0.001
HPMC-2	13.63 ± 0.006	46.51 ± 0.005	25 ± 0.007
HPMC-3	8.86 ± 0.006	56 ± 0.006	25.49 ± 0.003
HPMC/NFC-1	25.37 ± 0.014	59.52 ± 0.006	92.78 ± 0.056
HPMC/NFC-2	19.17 ± 0.019	40 ± 0.004	32.55 ± 0.004
HPMC/NFC-3	22.47 ± 0.013	36.98 ± 0.003	24.35 ± 0.01

UV-Vis Transmittance Studies of the HPMC/NFC Nanocomposite Films

The transmittance values for the commercial PVC (Cling film), the HPMC, and the HPMC/NFC films were measured using a UV-Vis spectrophotometer (Table 2). The transmittance value of the PVC was observed at 278 nm with a transmittance percent of 74%. The HPMC-1, HPMC-2, and HPMC-3 films had transmittance values of 275 nm, 275 nm, and 258 nm with transmission percentages of 72%, 64%, and 36%, respectively. Moreover, the transmittance values for the HPMC/NFC-1, HPMC/NFC-2, and HPMC/NFC-3 films were observed at 278, 274, and 274 nm with transmittance percentages of 32%, 29%, and 27%, respectively. The comparative transmittance values are shown in Fig. 3.

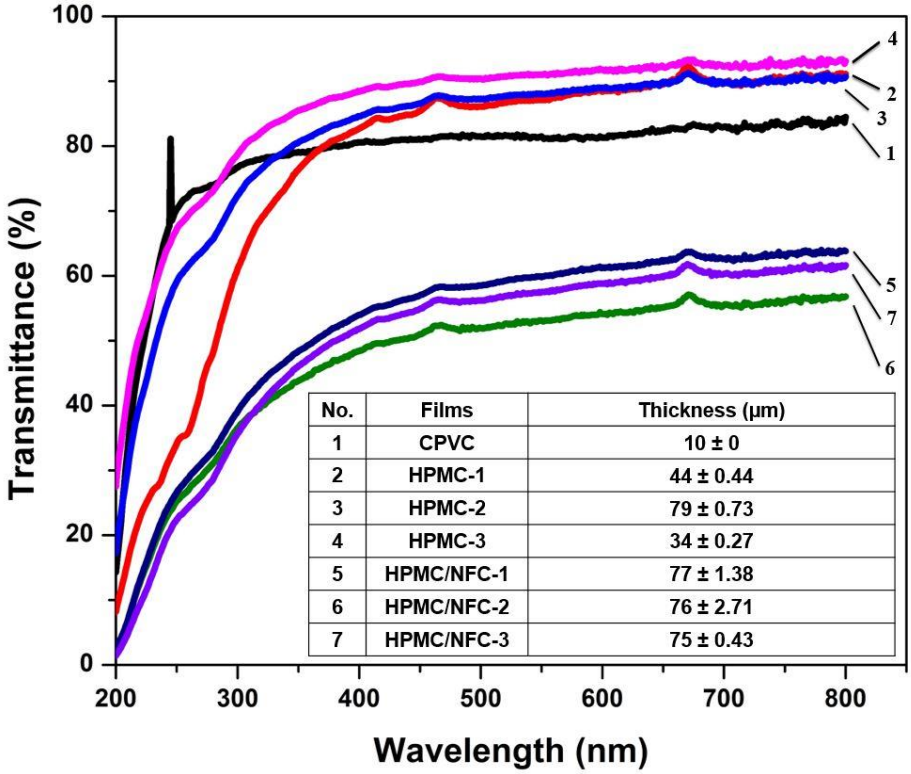

Fig. 3. UV-VIS transmittance studies of the commercial PVC, HPMC, and HPMC/NFC films

These results are in agreement with the work done by Lu *et al.* (2018) who studied transmittance spectra of BOPP/LDPE films. The untreated films were found with 86.3% and whereas NFC coated plasma-treated on BOPP/LDPE films with the value of 85.2%. Moreover, the films showed less transparency after the addition of NFC, and this may be explained because of nanofibrils and size effect (Fukuzumi *et al.* 2009; Aulin *et al.* 2010) The varying transmittance values may be attributed to the different concentrations of polymer and NFC in the films, which is supported by the SEM images. However, previous research has reported optical transparency values of approximately 90% in TEMPO-oxidized NFC cellulose films (Klemm *et al.* 2005). The films prepared from nanocellulose have high transparency values if the fibers are small enough between interstices to avoid light scattering (Fortunati *et al.* 2012). The UV-VIS transmittance properties may be affected due to the entanglement of fibers. This lower level of transmission upon the addition of NFC to the HPMC matrix is more suitable for designing biodegradable food

packaging material, where NFC in the film surface will cover the pores to better serve as a gas barrier. The NFC can also minimize the UV light-induced lipid oxidation on the skins of perishable fruits and vegetables while prolonging the storage life by a few days (Fortunati *et al.* 2012; Gopinathan *et al.* 2017). The nanocomposite film, which was successfully prepared by a combination of HPMC/NFC, had a uniform distribution of NFC with a size range between 216 nm to 551 nm. This may have been due to good processing, a smaller nano range size, and uniform distribution of the NFC into the polymer matrix compared to the HPMC films (2.6 µm to 14 µm), which was further evident compared to the PVC cling film (Ponni *et al.* 2020).

Table 2. UV-Vis Transmittance Values and Transmittance Percentages of the Commercial PVC, HPMC, and HPMC/NFC films

Sample	Transmittance Value (nm)	Transmittance (%)
CPVC	278	74
HPMC-1	275	72
HPMC-2	275	64
HPMC-3	258	36
HPMC/NFC-1	278	32
HPMC/NFC-2	274	29
HPMC/NFC-3	274	27

Rheological Behavior of the HPMC/NFC Nanocomposite Films

The rheological measurement of behavior has been the most common and efficient characterization method to study the polymer-based internal structure as well as the processing, evaluation, and feasibility of the nanocomposite film formulation. Meanwhile, data from the rheology study focused on the interactions between the polymers and the other appropriate ingredients. The rheological behavior of the composite HPMC and HPMC/NFC film formulations was studied for different concentrations of HPMC (1%, 2%, and 3%) at 30 °C, as seen in Fig. 4. All formulations of the composite HPMC and HPMC/NFC films showed a distinct shear-thinning behavior within the shear rate range of 1 s^{-1} to 100 s^{-1}. Similar results have been investigated and reported by Tang *et al.* (2014, 2018)**.** Moreover, there was no major difference between the samples. The HPMC/NFC-2 film had the highest shear viscosity at 33.55 Pa^{-s}, followed by the HPMC-3, HPMC/NFC-1, HPMC/NFC-3, HPMC-1, and HPMC-2 films, respectively. However, there was a slight decrease in the viscosity for HPMC/NFC-3 film in comparison with the HPMC-3 film. This may have been due to a strong dependence on a higher HPMC concentration and the incorporation of the NFC. Specifically, there is an increase in shear rate to $10s^{-1}$ for composite formulations from 2.65 Pa^{-s} in HPMC-1 to 3.58 Pa^{-s} in HPMC-3, whereas it showed a slight increase of 3.09 Pa^{-s} in HPMC/NFC-3 to 3.27 Pa^{-s} in HPMC/NFC-1 respectively. These results were consistent with previous research by Zhang *et al.* (2015), where the incorporation of NCC in polyvinylidene fluoride (PVDF) increased the shear viscosity of the sample. The findings from this study indicate that NFC acted as an effective thickening agent in the HPMC film formulation. The increased viscosity was attributed to strong interactions between the NFC and water, which is due to high polarity and an intrinsically large surface area. Thus, the NFC from *Agave americana* formed a network-like structure and exhibited a gel-forming behavior with high resistance to flow (Dimic-Misic *et al.* 2013; Mohtaschemi *et al.* 2014). In general, a higher viscosity is caused by the interaction of van der Waals forces. Although common with NFC and NCC, van der Waals

forces contribute to a higher viscosity in other common filler systems (Iyer *et al.* 2015a). In particular, the improvement of interfacial adhesion provides opportunities to form hydrogen bonds due to the high presence of hydroxyl groups in HPMC biopolymer and NFC. Finally, all the nanocomposite film formulations showed no major differences, but adding NFC did increase the viscosity in the shear rate range.

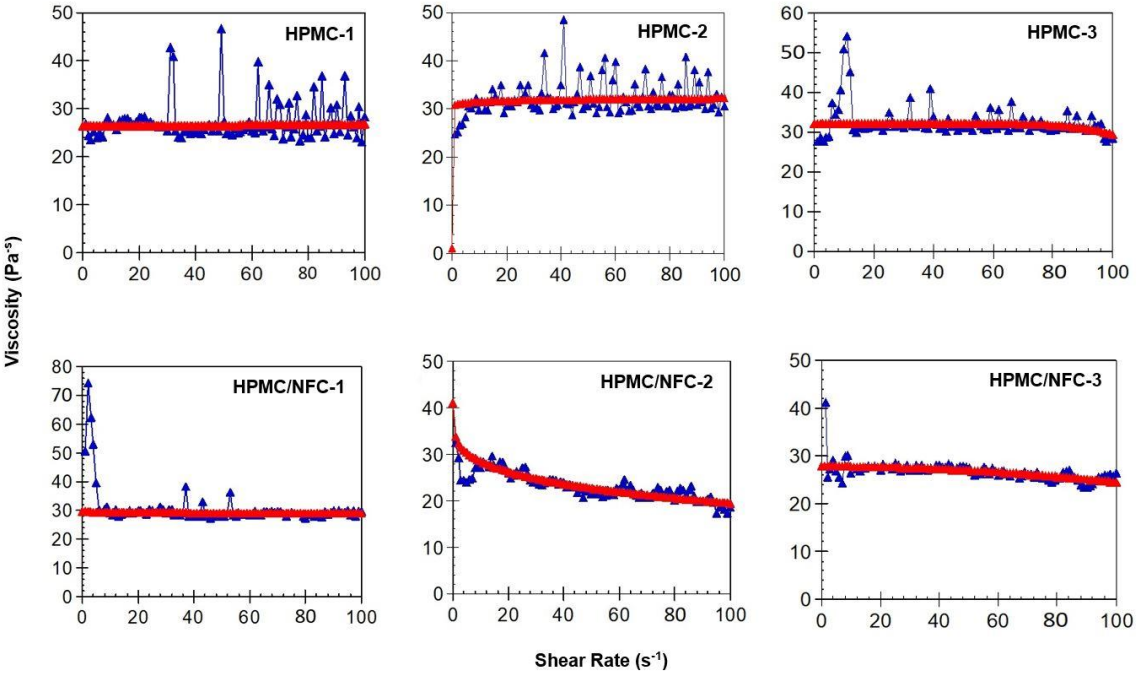

Fig. 4. The rheological behavior of the HPMC and HPMC/NFC formulations

Surface Morphology Studies of the HPMC/NFC Nanocomposite Films

Digital photographs of the HPMC and HPMC/NFC nanocomposites films are shown in Fig. 5 (a, b, c, d, e, f). The three nanocomposites prepared with the HPMC polymer were well blended with NFC and their surface morphologies were analyzed *via* SEM. All the nanocomposite films showed a uniform distribution with sizes ranging from 247 nm to 306 nm, 175 nm to 262 nm, and 292 nm to 845 nm for the HPMC/NFC-1, HPMC/NFC-2, and HPMC/NFC-3 films, respectively. The HPMC films without NFC showed some scattered aggregates with sizes of 4 µm to 11 µm, 1 µm to 5 µm, and 6 µm to 21 µm for the HPMC-1, HPMC-2, and HPMC-3 films, respectively (Fig. 6). The results were in agreement with those from the NFC/poly (vinyl alcohol) (PVA)/poly (acrylic acid)(PAA) nanofilms prepared from banana pseudostem (Ponni *et al.* 2020). Moreover, the average film thickness for HPMC-1, HPMC-2, HPMC-3, HPMC/NFC-1, HPMC/NFC-2, and HPMC/NFC-3 were 44, 79, 34, 77, 76, and 75 µm respectively. However, the addition of NFC to the polymer matrix showed great transparency, as well as significant changes with a uniform surface morphology of the films. The surface of the films without the NFC incorporation showed a smooth, intended polymer dispersion in the water (Dehnad *et al.* 2014). The light bumps on the surface of the films increased progressively due to the function of the NFC in the nanocomposite films, as can be seen in Fig. 5. Similar light bumps with NCC were observed in a study by Samir *et al.* (2005).

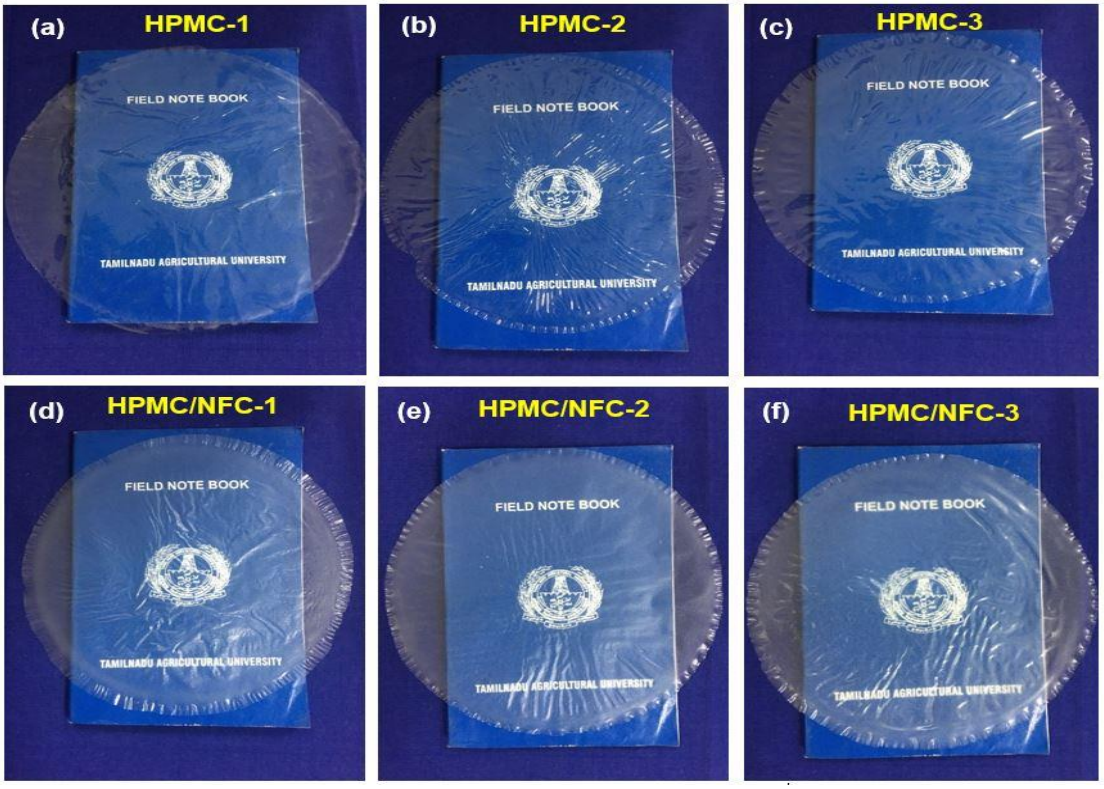

Fig. 5. Digital photos of the a) HPMC-1, b) HPMC-2, c) HPMC-3, d) HPMC/NFC-1, e) HPMC/NFC-2, and HPMC/NFC-3 nanocomposite films

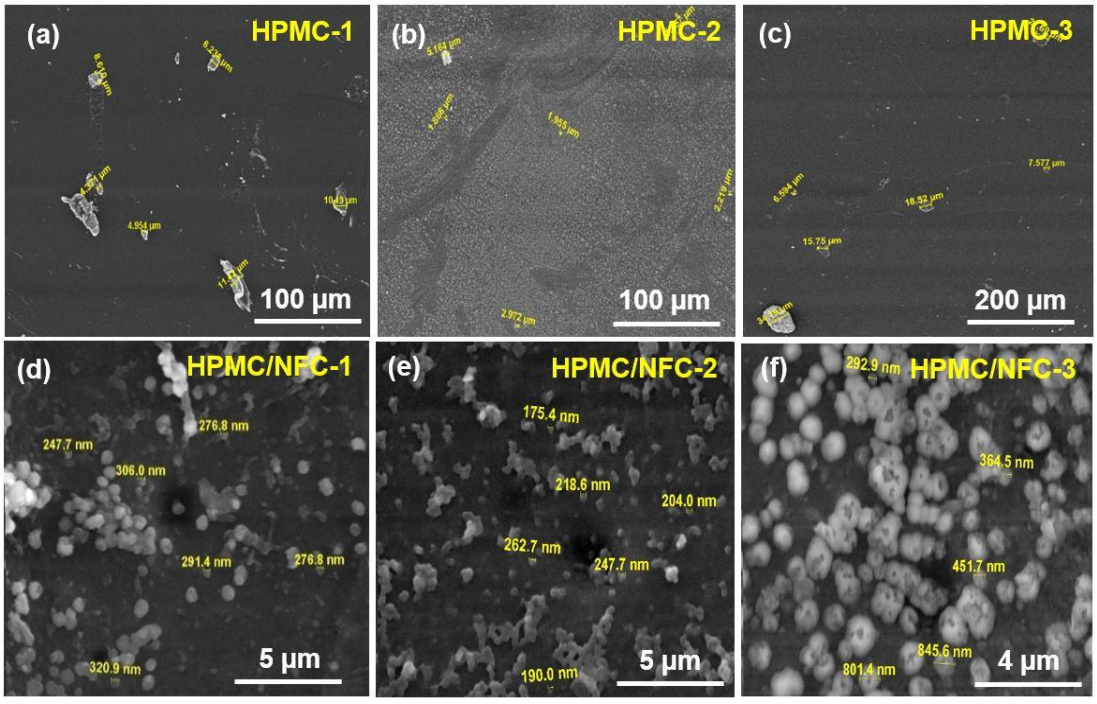

Fig. 6. SEM micrographs for the a) HPMC-1, b) HPMC-2, c) HPMC-3, d) HPMC/NFC-1, e) HPMC/NFC-2, and HPMC/NFC-3 nanocomposite films

FTIR Analysis of the HPMC/NFC Nanocomposite Films

Fourier transform infrared spectroscopy is a useful analysis for investigating and measuring the functional properties of materials. In this study, the films with or without the incorporation of the *Agave americana* NFC were recorded, and the results are shown in Fig. 7. For the HPMC films, absorbance maxima appeared in the range of 3407 to 3441 cm^{-1} with a maximum peak at 3441 cm^{-1} among the HPMC films. Similar results were outlined by Celebi and Kurt (2015) and Tang *et al.* (2018). These features correspond to OH vibration and NH stretching. Moreover, the symmetrical and asymmetrical peak shifts at 2922 cm^{-1} were attributed to CH stretching. The transmittance bands are recorded at the 1645 to 1652 cm^{-1} peak corresponding to the C=O stretching of the respective amide groups I and II. The C−O stretching vibration gives rise to a peak at 1044 cm^{-1}. The small peaks at 655 cm^{-1} are assigned to C−OH out of plane bending and similar results were reported by Krishnadev *et al.* (2020). The FTIR spectrum of the HPMC/NFC films exhibited sharp peaks at a range of 3345 to 3373 cm^{-1}, with the highest peak recorded at 3373 cm^{-1}. The peak at 3373 cm^{-1} was attributed to OH vibrations due to a strong intra-molecular bond of hydrogen. The strong peaks at 1037, 1037, and 1044 cm^{-1} are related to the C−O stretching at the C-3 position (Khan *et al.* 2012; Krishnadev *et al.* 2020). However, there was an increase in the HPMC/NFC FTIR spectra in comparison with the HPMC composite film samples. The peak value at 3373 cm^{-1} of the HPMC/NFC-3 composite film had a higher transmittance intensity than the HPMC films, which corresponded to hydrogen bonding between the HPMC and NFC (Khan *et al.* 2013). Meanwhile, there was a slight change to the peaks of the film samples without incorporating NFC. From these observations, the addition of NFC in the polymer matrix showed good interaction between the NFC and the polymer formulation, which can improve the overall mechanical strength of HPMC/NFC films plasticized with glycerol.

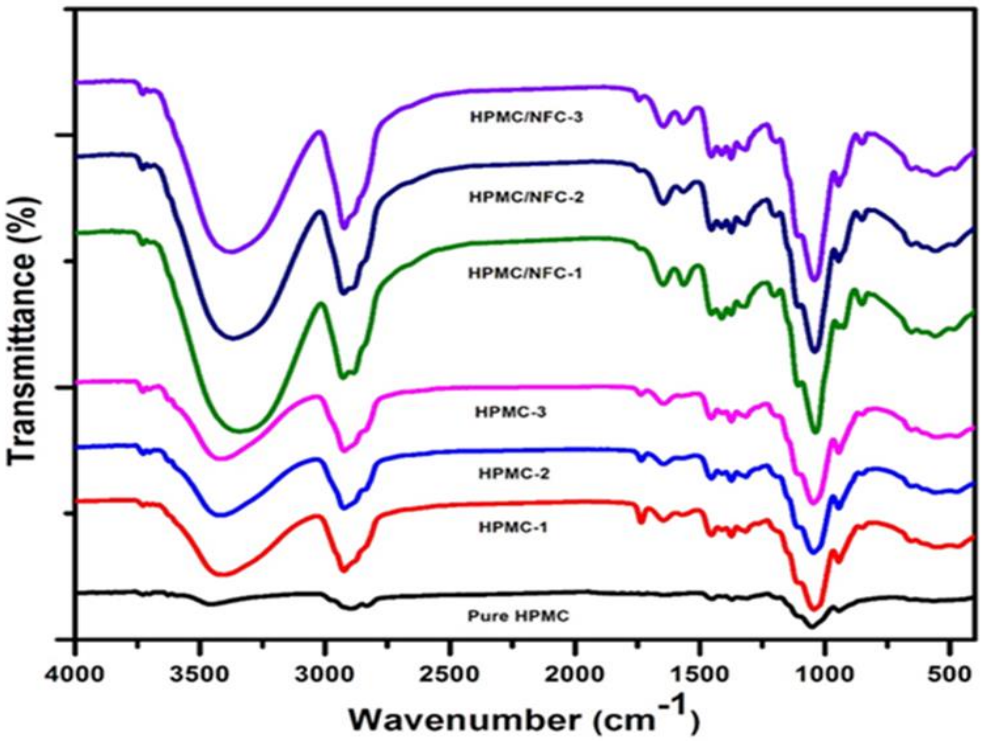

Fig. 7. FTIR spectra of the HPMC and HPMC/NFC nanocomposite films

XRD analysis of the HPMC/NFC Nanocomposite Films

The XRD profiles on the HPMC and HPMC/NFC composite films are shown in Fig. 8. The HPMC-1, HPMC-2, and HPMC-3 films had diffraction peaks of 2θ = 20.74°, 19.96°, and 20.35°, respectively. It was understood that the peak values are associated with the distinctive I structure of cellulose. Among all the peaks, there was an increase in the peak intensity at the beginning, followed by a decrease and then an increase in the intensity. The changes in the intensity are ascribed to the transformation of the structure from amorphous to crystalline. Another factor to consider was the HPMC/NFC nanocomposite films. The HPMC/NFC-1, HPMC/NFC-2, and HPMC/NFC-3 films had peaks at 2θ = 20.88°, 21.27°, and 21.27°, respectively. These peaks can be strongly related to the characteristic band of cellulose (Aulin *et al.* 2013) and it satisfactorily showed that there was a strong interaction between the two blended components which was confirmed through rheological studies. Similar findings for polylactic acid (PLA) and NFC in the PLA/starch/NFC biocomposites were observed by Mao *et al.* (2019). More specifically, the XRD patterns showed a peak increase from 273 with the HPMC film to 338, 348, and 402 with the HPMC/NFC at 1%, 2%, and 3% NFC, respectively. This increase may be due to the higher NFC content in the polymer matrix and the fact that all the diffraction patterns showed an increase in the peak intensity compared to the pure HPMC films. However, as more amorphous HPMC is introduced, the peak intensity of the HPMC/NFC films may show an overall decrease in the peak intensity (Luo *et al.* 2019).

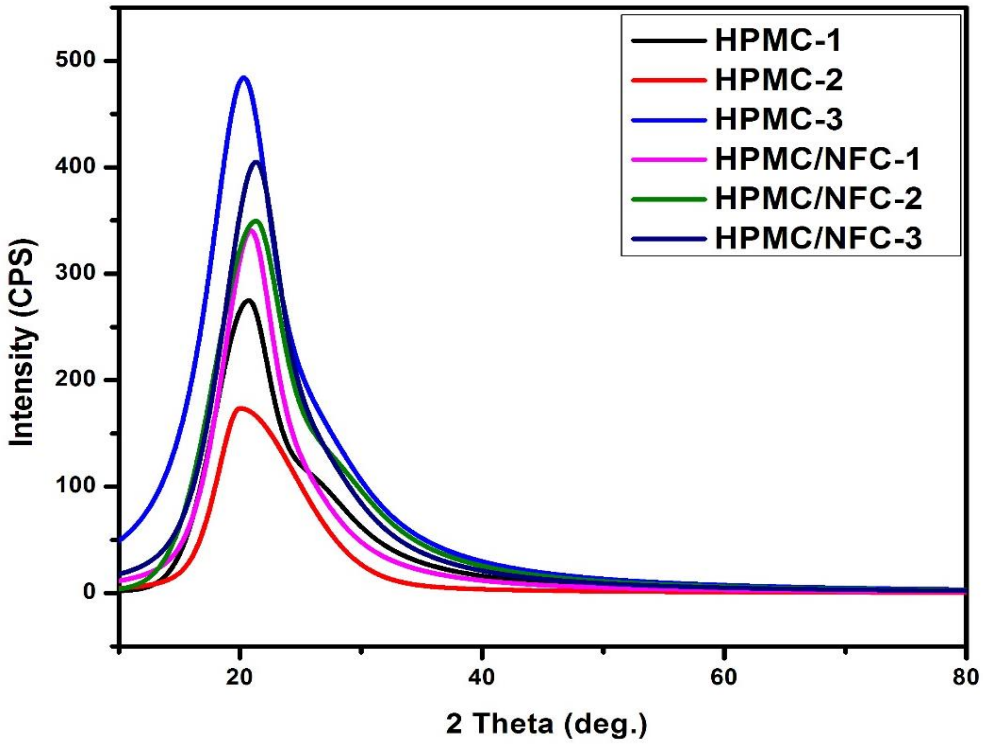

Fig. 8. XRD patterns of the HPMC and HPMC/NFC nanocomposite films

Thermal Analysis of the HPMC/NFC Nanocomposite Films

Derivative thermogravimetry (DTG) is a common thermal analysis technique common to TGA, which measures the weight loss at a weight increase with heating, cooling, or stable temperature. In general, DTG shows the process of decay or degradation

at various stages. The DTG curves for the HPMC films with and without the addition of NFC are shown in Fig. 9. The results showed that all the nanocomposite films were usually divided into three-stage degradation curves. The first part of the weight loss was due to the removal and evaporation of the solvent (water) at a temperature of 26 °C to 180 °C in the samples without incorporating NFC. These findings support similar research reported by Yang *et al.* (2014) and Tang *et al.* (2018). Moreover, water desorption and glycerol decomposition in the NFC-loaded polymer matrix were recorded at temperatures between 74 and 182 °C (Lassoued *et al.* 2021). In addition, the minor peaks in the curve were consistent with the degradation of the cellulose surface and internal structure (Roman and Winter 2004). The second mass loss in the film samples was found from 214 to 220 °C, which is attributed to the dehydration, deamination, depolymerization, and breakdown of the cellulose glycosidic linkages (Cao *et al.* 2009; Karakoti *et al.* 2020). Rapid weight loss above 370 °C is associated with oxidation and breakdown of char (Gopinathan *et al.* 2017; Tang *et al.* 2018; Krishnadev *et al.* 2020). Moreover, the HPMC/NFC films showed a decrease in thermal stability compared to the neat HPMC films. Consequently, the HPMC/NFC nanocomposite films showed a gradual and inevitable decrease of weight loss for an increase in NFC liquid suspension into the polymer matrix. However, there was a gradual change in weight loss percentage, because it showed a slight increase and then a complete decline in weight loss, which indicates a complete breakdown of NFC and other cellulose substitutes present in the films. Similar types of reinforced nanocomposites with NCC and NFC are reported in the literature (Celebi and Kurt 2015; Tang *et al.* 2018; Lassoued *et al.* 2021). Overall, NFC decreased the thermal degradation due to the resistance of the films to the higher temperature.

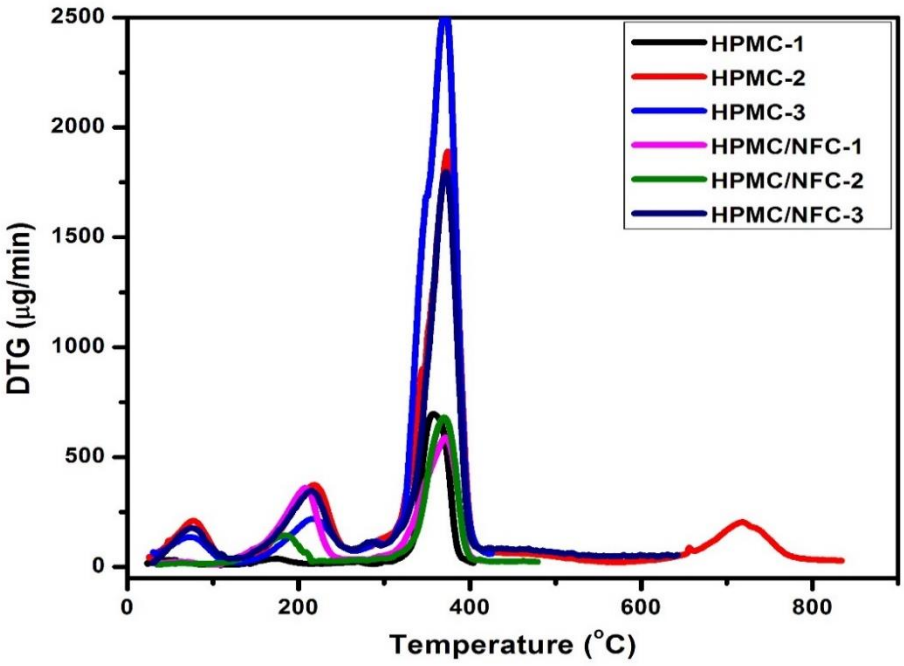

Fig. 9. The DTG curves of the HPMC and HPMC/NFC nanocomposite films

Mechanical Properties of the HPMC/NFC Nanocomposite Films.

The packaging films need adequate mechanical strength with good performance. Tensile strength is well connected to the mechanical strength of films, whereas the

elongation at break and young's modulus is related to the flexibility and rigidity of the films, respectively (Khan *et al.* 2014). Table 3 and Fig. 10 compare the mechanical properties of HPMC and HPMC/NFC nanocomposite films. In general, it was found that the HPMC films treated with 1% NFC had better TS properties compared to the HPMC/NFC-2 and HPMC/NFC-3 films (Fig. 10a).

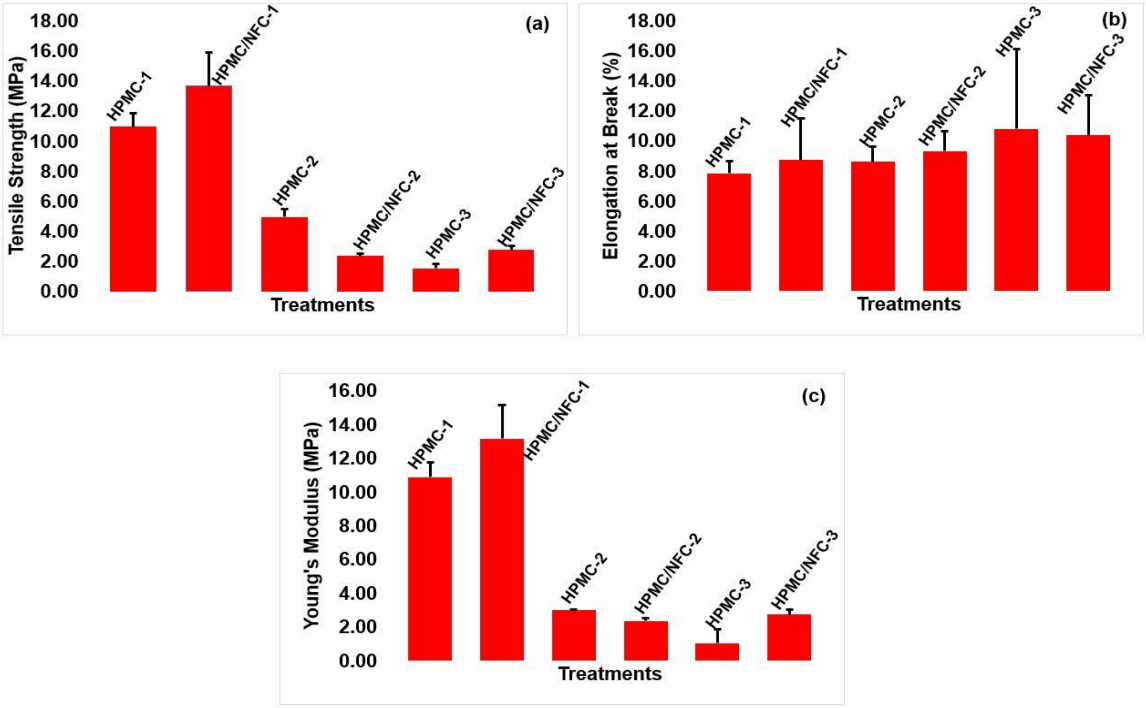

Fig. 10. The (a) TS, (b) EAB, and (c) YM values of the HPMC and HPMC/NFC nanocomposite films

The HPMC/NFC 1%, 2%, and 3% films had TS values of 13.68 MPa, 2.36 MPa, and 2.77 MPa, respectively. In addition, the EAB values increased moderately in all the films (Fig. 10b). However, the TS of the HPMC films decreased as the HPMC content increased. The HPMC 1%, 2%, and 3% films had TS values of 10.97 MPa, 4.96 MPa, and 1.54 MPa, respectively. It is well understood that the mechanical properties of the pure HPMC films exhibit brittleness and poor flexibility of the films. The use of a lower concentration (10 mL) of NFC with the HPMC imparted good TS and film flexibility properties. There was a gradual decrease in tensile strength, elongation at break (%), and Young's modulus by increasing the concentration of NFC in the HPMC nanocomposite films. The gain in the TS for the HPMC/NFC-1 sample represented a 24.6% increase compared to the other films. Lu *et al*. (2019) studied the addition of NFC on BOPP/LDPE on mechanical properties by assisting plasma treatment. The results revealed that plasma-treated BOPP/LDPE with and without NFC found no major mechanical difference as compared to untreated films. Aulin *et al.* (2013) reported that the addition of the NFC as a reinforcement material in the PLA matrix significantly increased the mechanical properties of the films. However, the TS values decreased after the nano fibrillated cellulose addition rate increased to 15 mL and 20 mL. This may have been due to the weakening of the nano fibrillated cellulose as reinforcement in the polymer matrix. Moreover, it was found that the YM value was 10.98 MPa in HPMC-1 film at 1%, which was then drastically reduced

to 3.41 MPa, and 1.22 MPa for the HPMC-2 and HPMC-3 samples, respectively. The HPMC/NFC nanocomposite films had YM values of 13.16, 3.66, and 2.73 MPa with respective NFC addition rates of 1%, 2%, and 3% (Fig. 9c). Therefore, the YM value of the HPMC/NFC-1 film was 16.56% higher than that of the HPMC-1 film. Similar results have been reported from related literature (Klangmuang and Sothornvit 2016; Tang *et al.* 2018). In addition, there was a negative effect on the EAB values with the addition of NFC to the composite samples, which was supported by findings in reported literature (Samir *et al.* 2004; Fortunati *et al.* 2015; Tang *et al.* 2018). The EAB values for the HPMC 1%, 2%, and 3% films were recorded with values of 7.87%, 8.60%, and 10.82%, respectively, while the EAB values for the HPMC/NFC films were recorded at 8.75%, 9.35%, and 10.40%, respectively. A change in the EAB values implies that adding NFC to the HPMC film showed good interaction between the filler and the matrix with moderate restriction of the matrix motion (Samir *et al.* 2004).

Table 3. Average TS, EAB, and YM Values of the HPMC, and HPMC/NFC films

Sample	TS (MPa)	EAB (%)	YM (MPa)
HPMC-1	11.0 ± 0.87	7.9 ± 0.99	10.9 ± 0.87
HPMC-2	5.0 ± 0.54	8.6 ± 0.86	3.4 ± 0.32
HPMC-3	1.5 ± 0.31	10.8 ± 5.33	1.1 ± 0.83
HPMC/NFC-1	13.7 ± 2.20	8.8 ± 2.76	13.2 ± 1.99
HPMC/NFC-2	2.4 ± 0.17	9.4 ± 1.34	2.4 ± 0.17
HPMC/NFC-3	2.8 ± 0.27	10.4 ± 2.65	2.7 ± 0.29

Gas Permeability of the HPMC/NFC Nanocomposite Films

The most fundamental requirement for any packaging material is "oxygen resistivity" which may help to trigger several changes in food such as deterioration of nutrients and prevent microbial growth, which overall influences the shelf life of packaged food products (Soni *et al*. 2016). One of the essential properties of food packaging is the need for a high-level oxygen barrier. For comparative OTR with the existing commercial packaging material is 1 to 10 cc/m^2·day for obtaining a good oxygen barrier (Abdellatief and Welt 2013). Other commercial packaging films prepared from polyethylene terephthalate/ polyethylene and (PET/PE) polyethylene terephthalate (PET) have been reported to be around 1.24 cc/m^2·day and 110 cc/m^2·day, respectively (Brody *et al.* 2008). In this study, the addition of NFC as reinforcement in three different concentrations of the HPMC polymer matrix was investigated. The results for gas permeability of O_2 through the films are shown in Fig. 11. The oxygen barrier in any composite film can improve the quality and help to stretch the shelf life of food (Sothornvit and Pitak 2007). Based on the findings, it is inferred that the amount of NFC in the HPMC polymer matrix showed a clear beneficial effect in decreasing the gas permeability of the film samples. The gas permeability of the HPMC-1 composite film was 67,840 mL/m^2·day, followed by HPMC-2 (101,620 mL/m^2·day) and HPMC-3 (122,049 mL/m^2·day). However, HPMC is very susceptible to oxygen permeability due to the presence of hydroxypropyl side groups, greater free volume, greater pores, lower crystallinity, and a lower cohesive energy density compared to similar cellulose-based materials like methylcellulose and ether (Miller and Krochta 1997). In addition, the 1%, 2%, and 3% reinforced HPMC/NFC matrix had gas permeability values of 17,415.5 (mL/m^2·day), 392.62 (mL/m^2·day), and 395.46 (mL/m^2·day), respectively. Compared to the pure HPMC films, the HPMC/NFC-1 nanocomposite films showed a 74.1% decrease in the O_2 permeability, followed by a 1,000-

fold decrease in the HPMC/NFC 2% and 3% films. This remarkable decrease in the gas permeability could be attributed to the imposition of the NFC and a reduction in the diffusion coefficient (Tang *et al.* 2018). These results are with the agreement of BOPP/LDPE/NFC films which displayed the lowest OTR (24.02 cc/m^2·day) (Lu *et al.* 2018). The main mechanism behind the gas permeability of the HPMC/NFC nanocomposite films is due to the inclusion of up to 3% of highly fibrillar material is likely to contribute only a few percentages of increase in the diffusion path of an oxygen molecule, assuming that is the only effect of the nanocellulose. It follows that the nanocellulose must be affecting the film structure. For instance, it may be preventing the formation of cracks in the film after it has been formed. The high entanglements are expected when stirred and tend to agglomerates depending upon their structural details. The NFC was also shown to close the pores in the film, which was revealed under the SEM with the dimensions from 247 to 306 nm, 175 to 262 nm, and 292 to 845 nm for the HPMC/NFC-1, HPMC/NFC-2, and HPMC/NFC-3 samples, respectively. According to chemistry, all nano-sized particles will display a higher surface-to-volume ratio, leading to high efficiency. The better interaction, crosslinking, and uniform distribution of NFC can reduce the gas barrier against air, O_2, and CO_2 through film sheets (Siró and Plackett 2010; Laxmeshwar *et al.* 2012; Ponni *et al.* 2020).

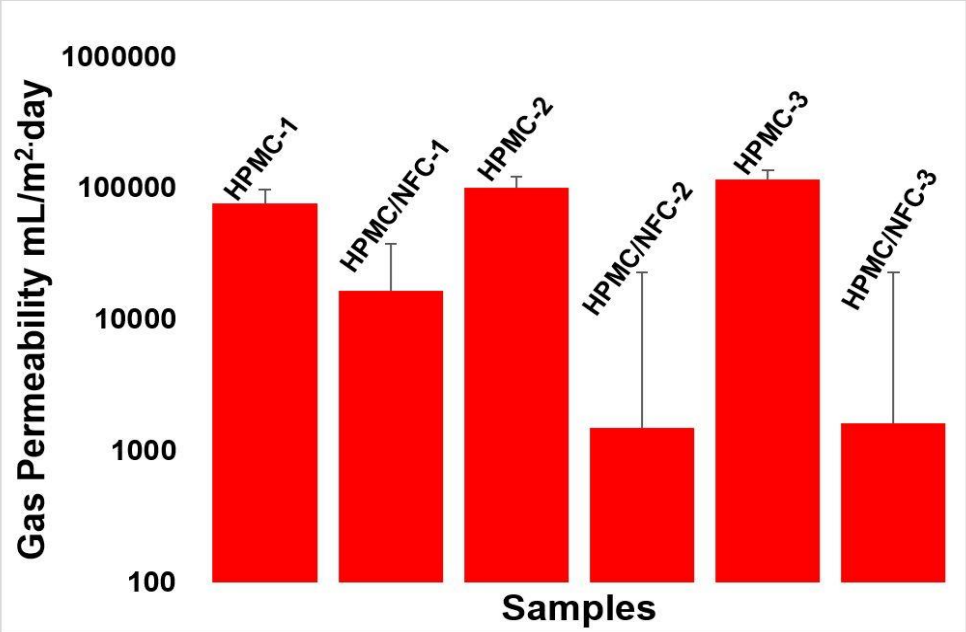

Fig. 11. The GPT results of the pure HPMC and HPMC/NFC samples

CONCLUSIONS

1. Nanofibrillated cellulose derived from succulent plant fiber *Agave americana* L was successfully used as a reinforcing composite material to develop highly transparent nanocomposite films.
2. The hydroxypropylmethylcellulose/ nanofibrillar cellulose (HPMC/NFC-1) film sample with 1% NFC addition had the best mechanical properties, the highest moisture content (25.4%), and the highest water solubility rate (59.5%).

3. The uniform dispersion, nano-sized dimensions, and good compatibility between the filler and matrix were confirmed by SEM.
4. The UV-Vis transmittance analysis showed a lower optical transmittance for all the HPMC/NFC films.
5. The gas transmission rates of the HPMC/NFC 2% and 3% samples showed a 1,000-fold reduction compared to their HPMC counterpart films.
6. The best biodegradability weight loss of 92.8% was observed in the HPMC/NFC-1 film sample buried in the soil for 15 d.
7. The prepared nanocomposite films are suitable for packaging wrapping material for preserving perishable fruits and vegetables as a protection from UV radiation.

ACKNOWLEDGMENTS

The authors are grateful to all for their technical assistance in carrying out this research work. The authors wish to thank K. S. Subramanian and A. Lakshmanan for their financial assistance in conducting experimental work from the DST-Nanomission pulses and EID-Parry schemes.

REFERENCES CITED

"The European Parliament and the Council of the European Union. Directive (EU) 2019/904 of the European parliament and of council of 5 June 2019 on the reduction of the impact of certain plastic products on the environment", *Off. J. Eur. Union* 2019, L155, 19

"The European Parliament and the Council of the European Union. Directive (EU) 2018/852 of the European parliament and of council of 30 May 2018 amending Directive 94/62/EC on packaging and packaging waste", *Off. J. Eur. Union* 2018, L150, 14.

Abdellatief, A., and Welt, B. A. (2013). "Comparison of new dynamic accumulation method for measuring oxygen transmission rate of packaging against the steady-state method described by ASTM D3985," *Packaging Technology and Science* 26(5), 281-288. DOI:10.1002/PTS.1974

ASTM D882-18 (2018). "Standard test method for tensile properties of thin plastic sheeting," ASTM International, West Conshohocken, PA.

Atikah, M. S. N., Ilyas, R. A., Sapuan, S. M., Ishak, M. R., Zainudin, E. S., Ibrahim, R., Atiqah, A., Ansari, M. N. M., and Jumaidin, R. (2019). "Degradation and physical properties of sugar palm starch/sugar palm nanofibrillated cellulose bionanocomposite," *Polimery* 64(10), 27-36. DOI: 10.14314/polimery.2019.10.5

Aulin, C., Gällstedt, M., and Lindström, T. (2010). "Oxygen and oil barrier properties of microfibrillated cellulose films and coatings," *Cellulose* 17(3), 559-574. DOI:10.1007/s10570-009-9393-y

Aulin, C., Karabulut, E., Tran, A., Wågberg, L., and Lindström, T. (2013). "Transparent nanocellulosic multilayer thin films on polylactic acid with tunable gas barrier properties," *ACS Applied Materials and Interfaces* 5(15), 7352-7359. DOI:

10.1021/am401700n

Brody, A. L., Bugusu, B., Han, J. H., Sand, C. K., and McHugh, T. H. (2008). "Innovative food packaging solutions," *Journal of Food Science* 73(8), 107-116. DOI:10.1111/J.1750-3841.2008.00933.X

Burdock, G. A. (2007). "Safety assessment of hydroxypropyl methylcellulose as a food ingredient," *Food and Chemical Toxicology* 45(12), 2341-2351. DOI: 10.1016/j.fct.2007.07.011

Cai, J., Liu, M., Wang, L., Yao, K., Li, S., and Xiong, H. (2011). "Isothermal crystallization kinetics of thermoplastic starch/poly(lactic acid) composites," *Carbohydrate Polymers* 86(2), 941-947. DOI: 10.1016/ j.carbpol.2011.05.044

Cao, X., Habibi, Y., and Lucia, L. A. (2009). "One-pot polymerization, surface grafting, and processing of waterborne polyurethane-cellulose nanocrystal nanocomposites," *Journal of Materials Chemistry* 19(38), 7137-7145. DOI: 10.1039/b910517d

Celebi, H., and Kurt, A. (2015). "Effects of processing on the properties of chitosan/cellulose nanocrystal films," *Carbohydrate Polymers* 133, 284-293. DOI: 10.1016/j.carbpol.2015.07.007

Chaabouni, Y., Drean, J.-Y., Msahli, S., and Sakli, F. (2006). "Morphological characterization of individual fiber of *Agave americana* L.," *Textile Research Journal* 76(5), 367-374. DOI: 10.1177/0040517506061965

Chandra, R., Takeuchi, H., and Hasegawa, T. (2012). "Methane production from lignocellulosic agricultural crop wastes: A review in context to second generation of biofuel production," *Renewable and Sustainable Energy Reviews* 16(3), 1462-1476. DOI: 10.1016/j.rser.2011.11.035

Cheng, L., Zhang, D., Gu, Z., Li, Z., Hong, Y., and Li, C. (2018). "Preparation of acetylated nanofibrillated cellulose from corn stalk microcrystalline cellulose and its reinforcing effect on starch films," *International Journal of Biological Macromolecules* 111, 959-966. DOI: 10.1016/j.ijbiomac.2018.01.056

Cui, S., Zhang, S., Ge, S., Xiong, L., and Sun, Q. (2016). "Green preparation and characterization of size-controlled nanocrystalline cellulose via ultrasonic-assisted enzymatic hydrolysis," *Industrial Crops and Products* 83, 346-352. DOI: 10.1016/j.indcrop.2016.01.019

De Souza Machado, A. A., Kloas, W., Zarfl, C., Hempel, S., and Rillig, M. C. (2018). "Microplastics as an emerging threat to terrestrial ecosystems," *Global Change Biology* 24(4), 1405-1416. DOI: 10.1111/gcb.14020

Dehnad, D., Mirzaei, H., Emam-Djomeh, Z., Jafari, S.-M., and Dadashi, S. (2014). "Thermal and antimicrobial properties of chitosan-nanocellulose films for extending shelf life of ground meat," *Carbohydrate Polymers* 109, 148-154. DOI: 10.1016/j.carbpol.2014.03.063

Dimic-Misic, K., Maloney, T., Liu, G., and Gane, P. (2017). "Micro nanofibrillated cellulose (MNFC) gel dewatering induced at ultralow-shear in presence of added colloidally-unstable particles," *Cellulose* 24(3), 1463-1481. DOI: 10.1007/s10570-016-1181-x

Dimic-Misic, K., Puisto, A., Gane, P., Nieminen, K., Alava, M. J., Paltakari, J., and Maloney, T. (2013). "The role of MFC/NFC swelling in the rheological behavior and dewatering of high consistency furnishes," *Cellulose* 20(6), 2847-2861. DOI: 10.1007/s10570-013-0076-3

Du, H., Liu, C., Mu, X., Gong, W., Lv, D., Hong, Y., Si, C., and Li, B. (2016). "Preparation and characterization of thermally stable cellulose nanocrystals via a sustainable approach of $FeCl_3$-catalyzed formic acid hydrolysis," *Cellulose* 23(4), 2389-2407. DOI: 10.1007/s10570-016-0963-5

Eurostat (2018). Available online: https://ec.europa.eu/eurostat/statistics explained/index.php/Packaging_waste_ statistics#Recycling_and_recovery_rates (accessed on 14 October 2021).

Ford, J. L. (1999). "Thermal analysis of hydroxypropylmethylcellulose and methylcellulose: Powders, gels and matrix tablets," *International Journal of Pharmaceutics* 179(2), 209-228. DOI: 10.1016/s0378-5173(98)00339-1

Fortunati, E., Luzi, F., Puglia, D., Petrucci, R., Kenny, J. M., and Torre, L. (2015). "Processing of PLA nanocomposites with cellulose nanocrystals extracted from *Posidonia oceanica* waste: Innovative reuse of coastal plant," *Industrial Crops and Products* 67, 439-447. DOI: 10.1016/j.indcrop.2015.01.075

Fortunati, E., Puglia, D., Monti, M., Peponi, L., Santulli, C., Kenny, J. M., and Torre, L (2012). "Extraction of cellulose nanocrystals from *Phormium tenax* fibres," *Journal of Polymers and the Environment* 21(2), 319-328. DOI: 10.1007/s10924-012-0543-1

Fukuzumi, H., Saito, T., Iwata, T., Kumamoto, Y., and Isogai, A. (2009). "Transparent and high gas barrier films of cellulose nanofibers prepared by TEMPO-mediated oxidation," *Biomacromolecules* 10(1), 162-165. DOI:10.1021/bm801065u

Gáspár, M., Benkő, Z., Dogossy, G., Réczey, K., and Czigány, T. (2005). "Reducing water absorption in compostable starch-based plastics," *Polymer Degradation and Stability* 90(3), 563-569. DOI: 10.1016/j.polymdegradstab.2005.03.012

Geyer, R., Jambeck, J. R., and Law, K. L. (2017). "Production, use, and fate of all plastics ever made," *Science Advances* 3(7), article no. e1700782. DOI: 10.1126/sciadv.1700782

Ghasemlou, M., Aliheidari, N., Fahmi, R., Shojaee-Aliabadi, S., Keshavarz, B., Cran, M. J., and Khaksar, R. (2013). "Physical, mechanical and barrier properties of corn starch films incorporated with plant essential oils," *Carbohydrate Polymers* 98(1), 1117-1126. DOI: 10.1016/j.carbpol.2013.07.026

Gopinathan, P., Subramanian, K. S., Paliyath, G., and Subramanian, J. (2017). "Genotypic variations in characteristics of nano-fibrillated cellulose derived from banana pseudostem," *BioResources* 12(4), 6984-7001, DOI: 10.15376/biores.12.4.6984-7001

Halimatul, M. J., Sapuan, S. M., Jawaid, M., Ishak, M. R., and Ilyas, R. A. (2019). "Effect of sago starch and plasticizer content on the properties of thermoplastic films: Mechanical testing and cyclic soaking-drying," *Polimery* 64(6), 422-431. DOI: 10.14314/polimery.2019.6.5

Hay, W. T., Fanta, G. F., Peterson, S. C., Thomas, A. J., Utt, K. D., Walsh, K. A., Boddu, V. M., and Selling, G. W. (2018). "Improved hydroxypropyl methylcellulose (HPMC) films through incorporation of amylose-sodium palmitate inclusion complexes," *Carbohydrate Polymers* 188, 76-84. DOI: 10.1016/j.carbpol.2018.01.088

Hosseini, S. N., Pirsa, S., and Farzi, J. (2021). "Biodegradable nano composite film based on modified starch-albumin/MgO; antibacterial, antioxidant and structural properties," *Polymer Testing* 97, 107182. DOI: 10.1016/j.polymertesting.2021.107182

Huang, J., Ma, X., Yang, G., and Alain, D. (2020). "Introduction to nanocellulose," in: *Nanocellulose: From Fundamentals to Advanced Materials*, J. Huang, D. Alain, and L. Ning (eds.), Wiley, pp. 1-20. DOI: 10.1002/9783527807437.ch1

Hui, L., Schadler, L. S., and Nelson, J. K. (2013). "The influence of moisture on the electrical properties of crosslinked polyethylene/silica nanocomposites," *IEEE Transactions on Dielectrics and Electrical Insulation* 20(2), 641-653. DOI: 10.1109/TDEI.2013.6508768.

Ibrahim, M. I. J., Sapuan, S. M., Zainudin, E. S., and Zuhri, M. Y. M. (2019). "Physical, thermal, morphological, and tensile properties of cornstarch-based films as affected by different plasticizers," *International Journal of Food Properties* 22(1), 925-941. DOI: 10.1080/10942912.2019.1618324

Ilyas, R. A., Sapuan, S. M., Ibrahim, R., Abral, H., Ishak, M. R., Zainudin, E. S., Atikah, M. S. N., Mohd Nurazzi, N., Atiqah, A., Ansari, M. N. M., *et al.* (2019). "Effect of sugar palm nanofibrillated cellulose concentrations on morphological, mechanical and physical properties of biodegradable films based on agro-waste sugar palm (*Arenga pinnata* (*Wurmb.*) *Merr*) starch," *Journal of Materials Research and Technology* DOI: 10.1016/j.jmrt.2019.08.028

Ilyas, R. A., Sapuan, S. M., Ishak, M. R., and Zainudin, E. S. (2018). "Development and characterization of sugar palm nanocrystalline cellulose reinforced sugar palm starch bionanocomposites," *Carbohydrate Polymers* 202, 186-202. DOI: 10.1016/j.carbpol.2018.09.002

ISO 15105-1 (2007). "Plastics – Film and sheeting – Determination of gas transmission rate – Part 1: Differential-pressure methods," International Organization for Standardization, Geneva, Switzerland.

Iyer, K. A., and Torkelson, J. M. (2015). "Importance of superior dispersion versus filler surface modification in producing robust polymer nanocomposites: The example of polypropylene/nanosilica hybrids," *Polymer* 68, 147-157. DOI: 10.1016/j.polymer.2015.05.015

Iyer, K. A., Flores, A. M., and Torkelson, J. M. (2015a). "Comparison of polyolefin biocomposites prepared with waste cardboard, microcrystalline cellulose, and cellulose nanocrystals via solid-state shear pulverization," *Polymer* 75, 78-87. DOI: 10.1016/j.polymer.2015.08.029

Iyer, K. A., Schueneman, G. T., and Torkelson, J. M. (2015b). "Cellulose nanocrystal/ polyolefin biocomposites prepared by solid-state shear pulverization: Superior dispersion leading to synergistic property enhancements," *Polymer* 56, 464-475. DOI: 10.1016/j.polymer.2014.11.017

Karakoti, A., Biswas, S., Aseer, J. R., Sindhu, N., and Sanjay, M. R. (2020). "Characterization of microfiber isolated from *Hibiscus sabdariffa* var. *altissima* fiber by steam explosion," *Journal of Natural Fibers* 17(2), 189-198. DOI: 10.1080/15440478.2018.1477085

Kavoosi, G., Dadfar, S. M. M., and Purfard, A. M. (2013). "Mechanical, physical, antioxidant, and antimicrobial properties of gelatin films incorporated with thymol for potential use as nano wound dressing," *Journal of Food Science* 78(2), E244-E250. DOI: 10.1111/1750-3841.12015

Khan, A., Khan, R. A., Salmieri, S., Tien, C. L., Riedl, B., Bouchard, J., Chauve, G., Tan, V., Kamal, M. R., and Lacroix, M. (2012). "Mechanical and barrier properties of nanocrystalline cellulose reinforced chitosan based nanocomposite films," *Carbohydrate Polymers* 90(4), 1601-1608. DOI: 10.1016/j.carbpol.2012.07.037

Khan, R. A., Beck, S., Dussault, D., Salmieri, S., Bouchard, J., and Lacroix, M. (2013). "Mechanical and barrier properties of nanocrystalline cellulose reinforced poly(caprolactone) composites: Effect of gamma radiation," *Journal of Applied Polymer Science* 129(5), 3038-3046. DOI: 10.1002/app.38896

Khan, A., Salmieri, S., Fraschini, C., Bouchard, J., Riedl, B., and Lacroix, M. (2014). "Genipin cross-linked nanocomposite films for the immobilization of antimicrobial agent," *ACS Applied Materials & Interfaces* 6(17), 15232-15242. DOI: 10.1021/am503564m

Kim, H.-Y., Jane, J.-L., and Lamsal, B. (2017). "Hydroxypropylation improves film properties of high amylose corn starch," *Industrial Crops and Products* 95(4) 175-183. DOI: 10.1016/j.indcrop.2016.10.025

Klangmuang, P., and Sothornvit, R. (2016). "Combination of beeswax and nanoclay on barriers, sorption isotherm and mechanical properties of hydroxypropyl methylcellulose-based composite films," *LWT - Food Science and Technology* 65, 222-227. DOI: 10.1016/j.lwt.2015.08.003

Klemm, D., Heublein, B., Fink, H.-P., and Bohn, A. (2005). "Cellulose: Fascinating biopolymer and sustainable raw material," *Angewandte Chemie (International Edition)* 44(22), 3358-3393. DOI: 10.1002/anie.200460587

Krishnadev, P., Subramanian, K. S., Janavi, G. J., Ganapathy, S., and Lakshmanan, A. (2020). "Synthesis and characterization of nano-fibrillated cellulose derived from green *Agave americana* L. fiber," *BioResources* 15(2), 2442-2458. DOI: 10.15376/biores.15.2.2442-2458

Laksmana, F. L., Kok, P. J. A. H., Vromans, H., and Van der Voort Maarschalk, K. (2009). "Predicting the diffusion coefficient of water vapor through glassy HPMC films at different environmental conditions using the free volume additivity approach," *European Journal of Pharmaceutical Sciences* 37(5), 545-554. DOI:10.1016/j.ejps.2009.04.011

Lassoued, M., Crispino, F., and Loranger, E. (2021). "Design and synthesis of transparent and flexible nanofibrillated cellulose films to replace petroleum-based polymers," *Carbohydrate Polymers* 254, article no. 117411. DOI: 10.1016/j.carbpol.2020.117411

Laxmeshwar, S. S., Kumar, D. J. M., Viveka, S., and Nagaraja, G. K. (2012). "Preparation and properties of biodegradable film composites using modified cellulose fibre-reinforced with PVA," *ISRN Polymer Science* article no. 154314, 1-8. DOI: 10.5402/2012/154314

Li, Y., Liu, Y., Chen, W., Wang, Q., Liu, Y., Li, J., and Yu, H. (2016). "Facile extraction of cellulose nanocrystals from wood using ethanol and peroxide solvothermal pretreatment followed by ultrasonic nanofibrillation," *Green Chemistry* 18(4), 1010-1018. DOI: 10.1039/c5gc02576a

Lu, P., Guo, M., Xu, Z., and Wu, M. (2018). "Application of nanofibrillated cellulose on BOPP/LDPE film as oxygen barrier and antimicrobial coating based on cold plasma treatment," *Coatings*, 8(6), 207. DOI:10.3390/coatings8060207

Luo, K., Wang, Y., Xiao, H., Song, G., Cheng, Q., and Fan, G. (2019). "Preparation of convertible cellulose from rice straw using combined organosolv fractionation and alkaline bleaching," *IOP Conference Series: Earth and Environmental Science* 237(5), 1-6. DOI: 10.1088/1755-1315/237/5/052053

Lv, S., Zhang, Y., Gu, J., and Tan, H. (2018). "Physicochemical evolutions of starch/poly (lactic acid) composite biodegraded in real soil," *Journal of Environmental Management* 228, 223-231. DOI: 10.1016/ j.jenvman.2018.09.033

Mao, J., Tang, Y., Zhao, R., Zhou, Y., and Wang, Z. (2019). "Preparation of nanofibrillated cellulose and application in reinforced PLA/starch nanocomposite film," *Journal of Polymers and the Environment* 27(4), 728-738. DOI: 10.1007/s10924-019-01382-6

Maran, J. P., Sivakumar, V., Thirugnanasambandham, K., and Sridhar, R. (2014). "Degradation behavior of biocomposites based on cassava starch buried under indoor soil conditions," *Carbohydrate Polymers* 101, 20-28. DOI: 10.1016/j.carbpol.2013.08.080

Marichelvam, M. K., Jawaid, M., and Asim, M. (2019). "Corn and rice starch-based bio-plastics as alternative packaging materials," *Fibers* 7(4), 32. DOI: 10.3390/fib7040032

McGinity, J. W., and Felton, L. A. (2008). *Aqueous Polymeric Coatings for Pharmaceutical Dosage Forms*, CRC Press, Boca Raton, FL.

Miller, K. S., and Krochta, J. M. (1997). "Oxygen and aroma barrier properties of edible films: A review," *Trends in Food Science & Technology* 8(7), 228-237. DOI: 10.1016/S0924-2244(97)01051-0

Mohtaschemi, M., Dimic-Misic, K., Puisto, A., Korhonen, M., Maloney, T., Paltakari, J., and Alava, M. J. (2014). "Rheological characterization of fibrillated cellulose suspensions via bucket vane viscometer," *Cellulose* 21(3), 1305-1312. DOI: 10.1007/s10570-014-0235-1

Mondal, S. (2018). "Review on nanocellulose polymer nanocomposites," *Polymer-Plastics Technology and Engineering* 57(13), 1377-1391. DOI:10.1080/03602559.2017.1381253

Msahli, S., Jaouadi, M., Sakli, F., and Drean, J.-Y. (2015). "Study of the textile potential of fibres extracted from Tunisian *Agave americana* L.," *Journal of Natural Fibers* 12(6), 552-560. DOI: 10.1080/15440478.2014.984046

Navarro-Tarazaga, M. L., del Río, M. A., Krochta, J. M., and Pérez-Gago, M. B. (2008). "Fatty acid effect on hydroxypropyl methylcellulose-beeswax edible film properties and postharvest quality of coated 'ortanique' mandarins," *Journal of Agricultural and Food Chemistry* 56(22), 10689-10696. DOI: 10.1021/jf801967q

Ponni, P., Subramanian, K. S., Janavi, G. J., and Subramanian, J. (2020). "Synthesis of nano-film from nanofibrillated cellulose of banana pseudostem (*Musa* spp.) to extend the shelf life of tomatoes," *BioResources* 15(2), 2882-2905. DOI: 10.15376/biores.15.2.2882-2905

Preechawong, D., Peesan, M., Supaphol, P., and Rujiravanit, R. (2005). "Preparation and characterization of starch/poly(L-lactic acid) hybrid foams," *Carbohydrate Polymers* 59(3), 329-337. DOI: 10.1016/j.carbpol.2004.10.003

Ramesh, M., Palanikumar, K., and Reddy, K. H. (2017). "Plant fibre based bio-composites: Sustainable and renewable green materials," *Renewable and Sustainable Energy Reviews* 79, 558-584. DOI: 10.1016/j.rser.2017.05.094

Roman, M., and Winter, W. T. (2004). "Effect of sulfate groups from sulfuric acid hydrolysis on the thermal degradation behavior of bacterial cellulose," *Biomacromolecules* 5, 1671-1677. DOI: 10.1021/bm034519

Samir, M. A. S. A., Alloin, F., and Dufresne, A. (2005). "Review of recent research into cellulosic whiskers, their properties and their application in nanocomposite field," *Biomacromolecules* 6(2), 612-626. DOI: 10.1021/bm0493685

Samir, M. A. S. A., Alloin, F., Sanchez, J.-Y., and Dufresne, A. (2004). "Cellulose nanocrystals reinforced poly(oxyethylene)," *Polymer* 45(12), 4149-4157. DOI: 10.1016/j.polymer.2004.03.094

Sangroniz, A., Zhu, J. B., Tang, X., Etxeberria, A., Chen, E. Y. X., and Sardon, H. (2019). "Packaging materials with desired mechanical and barrier properties and full chemical recyclability," *Nature Communications* 10(1), 1-7. DOI:10.1038/s41467-019-11525-x

Sanyang, M. L., Ilyas, R. A., Sapuan, S. M., and Jumaidin, R. (2017). "Sugar palm starch-based composites for packaging applications," in: *Bionanocomposites for Packaging Applications*, M. Jawaid, and S. K. Swain (eds.), Springer International Publishing, Basel, Switzerland, pp. 125-147.

Siró, I., and Plackett, D. (2010). "Microfibrillated cellulose and new nanocomposite materials: A review," *Cellulose* 17(3), 459-494. DOI: 10.1007/s10570-010-9405-y

Soni, B., Schilling, M. W., and Mahmoud, B. (2016). "Transparent bionanocomposite films based on chitosan and TEMPO-oxidized cellulose nanofibers with enhanced mechanical and barrier properties," *Carbohydrate Polymers* 151, 779-789. DOI:10.1016/j.carbpol.2016.06.022

Sothornvit, R., and Pitak, N. (2007). "Oxygen permeability and mechanical properties of banana films," *Food Research International* 40(3), 365-370. DOI: 10.1016/j.foodres.2006.10.010

Tang, Y., Yang, S., Zhang, N., and Zhang, J. (2014). "Preparation and characterization of nanocrystalline cellulose via low-intensity ultrasonic-assisted sulfuric acid hydrolysis," *Cellulose* 21(1), 335-346. DOI: 10.1007/s10570-013-0158-2

Tang, Y., Zhang, X., Zhao, R., Guo, D., and Zhang, J. (2018). "Preparation and properties of chitosan/guar gum/nanocrystalline cellulose nanocomposite films," *Carbohydrate Polymers* 197, 128-136. DOI: 10.1016/j.carbpol.2018.05.073

Wang, C., Huang, H., Jia, M., Jin, S., Zhao, W., and Cha, R. (2015). "Formulation and evaluation of nanocrystalline cellulose as a potential disintegrant," *Carbohydrate Polymers* 130, 275-279. DOI: 10.1016/j.carbpol.2015.05.007

Yang, L., Lu, S., Li, J., Zhang, F., and Cha, R. (2015). "Nanocrystalline cellulose-dispersed AKD emulsion for enhancing the mechanical and multiple barrier properties of surface-sized paper," *Carbohydrate Polymers* 136, 1035-1040. DOI: 10.1016/j.carbpol.2015.10.011

Yang, S., Tang, Y., Wang, J., Kong, F., and Zhang, J. (2014). "Surface treatment of cellulosic paper with starch-based composites reinforced with nanocrystalline cellulose," *Industrial & Engineering Chemistry Research* 53(36), 13980-13988. DOI: 10.1021/ie502125s

Zhang, Z., Wu, Q., Song, K., Lei, T., and Wu, Y. (2015). "Poly(vinylidene fluoride)/ cellulose nanocrystals composites: Rheological, hydrophilicity, thermal and mechanical properties," *Cellulose* 22(4), 2431-2441. DOI: 10.1007/s10570-015-0634-y

Article submitted: September 1, 2021; Peer review completed: October 4, 2021; Revised version received and accepted: October 16, 2021; Published: October 20, 2021.
DOI: 10.15376/biores.16.4.8125-8151